REMARKS

The Examiner is correct that the preambles of claims 76-82 and 85-91 were incorrect and this has been addressed by amendment. This aspect of the rejection under 35 U.S.C. 112, second paragraph is therefore moot.

Rejection of Claim 84 Under 35 U.S.C. 112, Second Paragraph

First, objection was made to the use of the trademark/trade name "Nafion" as an assertedly inappropriate identifier citing *Ex parte Simpson*, 218 USPQ 1020 (Bd. App. 1982). While the Examiner is correct that in many instances, the use of a trademark or trade name cannot be used properly to identify a particular material or product, in the present case, this general statement is inappropriate. First, although Nafion is a trademark, "Nafion 117" refers to a specific material. Nafion 117, as used in the present instance, has a clear meaning in the art. A straightforward Google search for this term yields 96,000 hits, the first ten of which are reprinted as Exhibit A. Also included in Exhibit A are sample reprints which demonstrate the use of Nafion 117 as a generic term whose meaning is well understood. These include Sheppard, S-A, *et al.*, *The Analyst* (1998) 123:1923-1929, which describes the use of Nafion 117 as substrate for platinum coating, an abstract by Steward, F.F., *et al.*, from a 2005 annual meeting of the American Institute of Chemical Engineering, and a blog from "Auto," which refers specifically to Nafion 117. This is in contrast to the facts in *Simpson* wherein "Hypalon," which was used in a claim to refer to chlorosulfonated ethylene, was considered unclear. The problem, according to *Simpson*, was that the scope of the claim could not be determined because it was unclear whether the term "Hypalon" referred to a particular product or to any chlorosulfonated ethylene or to any synthetic resin as asserted by the applicant. No such assertion is being made here.

In any case, regardless of whether Nafion 117 is or is not an appropriate descriptor, it is unnecessary to evaluate the scope of that term in the context of claim 84. Nafion 117 is not used as a descriptor of a claimed element; rather, it refers to a labeled portion of the graph depicting the relationship of the thickness of a layer of a particular material to area-specific resistance. The position of Nafion 117 on the graph is clearly shown. It would not matter if this material were

named "Charlie" or "Fred," the range of area-specific resistance (ASR) is clearly shown in the diagram. Accordingly, this aspect of the rejection may be withdrawn.

Claim 84 is further rejected based on the assertion that the use of an illustrative table/figure is improper. The basis for this, that "incorporation by reference to a specific figure or table is inappropriate except under certain circumstance," is inapposite here. The figure is not incorporated by reference. It is set forth specifically in the claim. The citation of *Ex parte Fressola*, 27 USPQ2d 1608, 1609 (Bd. Pat. App. & Inter. 1993) is illustrative of the type of claim that is not permitted except in certain circumstances. The claim in that case was directed to:

> A system for the display of stereographic three-dimensional images of celestial objects as disclosed in the specification and drawings herein.

Applicant would not question that the claim in *Fressola* is inherently unclear. In its decision, the Board discusses at length a prior practice of permitting claims of this type, this practice having been superseded by the requirement for a more definite claim language especially after the passage of the statute in 1952. As the Board pointed out, this claim requires gleaning by analysis of all of the figures and all of the specification what the invention is.

Fressola is a far cry from the situation in the present case. The drawing is set forth specifically in the claim and no analysis is required.

Applicant appreciates the acknowledgment that claims 75-82 clearly set forth the scope of the invention; however, as applicant is entitled to claim his invention as he sees fit, and as the language of claim 84 is proper, it is believed that the rejection of this claim under 35 U.S.C. 112, second paragraph, is inappropriate.

Finally, the assertion that the figure is "subject to multiple interpretations" is not understood. The range of ASR for Nafion 117 shown in the figure is clearly readable.

Rejection Over Baucke, *et al.*

Claims 75-76, 80-81, 84-85 and 89-90 were rejected under 35 USC §§ 102(b)/103 over Baucke, *et al.*, U.S. Patent No. 5,094,927. The present RCE was filed in order to amend the claims to avoid what appeared to be an accidental anticipation by Baucke. Specifically, the claims were amended to specify that the proton-conducting membrane "consists essentially of a *single* metal or metal hydride support." This is shown as the proton-conducting membrane which corresponds, for example, to item 6.4 in figure 6 of the present application. As seen in figure 6, the anode and cathode (6.3 and 6.5) flank the proton-conducting membrane that has a single metal or metal hydride support represented as 6.4, which is the subject of the present claims.

In contrast, the example in Baucke referred to by the Examiner contains not a single, but two metal layers, which are actually the electrodes bracketing an electrolyte that has no metal support.

There is no illustration or disclosure in Baucke of a proton-conducting membrane with a single metal or metal hydride support. As shown in figure 2, which is the subject of the example, layer 11 is the nickel layer which is an oxygen electrode; layers 13 and 14 are the hydrogen electrode composed of a nickel layer coated onto platinum. The electrolyte itself, Ta_2O_5, is thus bracketed by two metal sheets.

Any anticipation by Baucke, thus, was coincidental in the first place as the metal layers performed as electrodes, not as supports for the electrolyte. This coincidental possible anticipation was deliberately amended out of the claims by requiring only a single metal or metal hydride support. Baucke always shows at least two metals bracketing the electrolyte.

Applicant is aware that claiming an inherent property of a composition or article of manufacture that is already disclosed in the art does not render the subject matter patentable. However, that is not the case here, since the claims as amended to require only a single metal or metal hydride support with the closed language "consisting essentially of" are not anticipated even coincidentally by Baucke.

Rejection Under 35 USC 103 Over Smotkin, *et al.* Combined With Various Secondary Documents

All claims were rejected on the basis of the combination of Smotkin, *et al.*, 5,846,669 in view of any one of several secondary documents which the Office characterizes as Norby, Crome, Kwang, and Dorthe.

This rejection appears to be a verbatim repetition of the rejections previously made on 8 August 2005 prior to several significant claim amendments and were fully responded to in the Response filed 9 January 2006. The contents of that Response are incorporated herein. However, applicant briefly points out that Smotkin is inappropriate as a primary reference since the Smotkin disclosure requires the presence of a liquid-containing electrolyte and the present claims require that the inorganic material "contains no liquid phase."

Rejection Under 35 USC 103 Over WO 98/21777 With Various Secondary Documents

Similarly, this basis for rejection is verbatim from that initially issued 8 August 2005 prior to several amendments to the claims. It has been fully responded to the in the response of 9 January 2006, and the contents of that response along with the accompanying declaration are incorporated. Briefly, however, the '777 document has only an abstract in English and corresponds to U.S. Patent No. 6,242,122. As noted, the primary document fails to disclose the required limitations of the present claims that the proton-conducting membrane contains no liquid phase and consists of only inorganic materials. Accordingly, its combination with secondary documents which simply disclose specific materials is inappropriate.

Regarding Response to Arguments

Regarding "Response to Arguments," applicant agrees that his response to the rejections has not changed substantially with regard to those previously presented. It is not understood why these are moot in view of the new rejection as the prior ones have been maintained. Response is provided herein to the new grounds for rejection as set forth above.

With regard to the remainder of the "Response to Arguments," like the rejections based on Smotkin and '777, these are verbatim repetitions of contentions to which applicant has already responded on 24 May 2006 to the points reviewed in paragraphs 21-29 on pages 31-35 and to the remaining sections 1-4 on pages 35-38 and paragraphs 1-21 on pages 38-45 in previous responses after these "Response to Arguments" were first asserted. Applicant sees no need to repeat this subject matter.

Conclusion

As noted, a Request for Continued Examination was filed in this application rather than filing a Notice of Appeal in order to amend the claims to avoid what appeared to be a coincidental anticipation by Baucke, *et al.*, a document that was of record, but apparently not appreciated by either applicant or the Examiner prior to the Examiner's attention being called to it in the Response to final Office action filed 24 May 2006. Baucke, *et al.* was cited in an IDS received at the USPTO on 10 October 2003 and acknowledged by the Examiner on 26 January 2004. As noted in the 24 May 2006 Response, the relevance of this document did not become apparent to applicant until the coincidental construction features were pointed out in a non-U.S. counterpart. In order to accommodate this, an RCE was filed in order to amend the claims.

Applicant acknowledges that the remaining bases for rejections have been fully argued on the record and are prepared to contest the position of the Examiner on appeal.

In the event the U.S. Patent and Trademark office determines that an extension and/or other relief is required, applicant petitions for any required relief including extensions of time and authorizes the Commissioner to charge the cost of such petitions and/or other fees due in connection

with the filing of this document to **Deposit Account No. 03-1952** referencing docket no. **491712000100**. However, the Commissioner is not authorized to charge the cost of the issue fee to the Deposit Account.

Dated: October 27 2006

Respectfully submitted,

By Kate H. Murashige

Kate H. Murashige
Registration No.: 29,959
MORRISON & FOERSTER LLP
12531 High Bluff Drive, Suite 100
San Diego, California 92130-2040
(858) 720-5112

Web

Results 1 - 10 of about 96,000 for nafion 117. (0.05 seconds)

[PDF] Application Notes
File Format: PDF/Adobe Acrobat - View as HTML
Nafion 117 films under various humidity condi- ... Figure 6 shows the mass gain of **Nafion 117** ... havior of the **Nafion 117** film under three differ- ...
www.rigakumsc.com/journal/Vol21.1.2004/rj21106.pdf - Similar pages

Fuel Cell Membrane Shootout Showcases Hydrocarbon Superiority ...
In the shootout, which PolyFuel calls the "DMFC Challenge Demo," the PolyFuel hydrocarbon DMFC membrane and the **Nafion 117** membrane have been built into ...
www.theautochannel.com/news/2004/11/01/268229.html - 25k - Cached - Similar pages

Stability and Performance of **Nafion-117** Membranes for the ...
Recent efforts at the INL have concentrated on applying pervaporation through **Nafion-117** membranes for the removal of water from HI/water and ...
aiche.confex.com/aiche/2005/techprogram/P13921.HTM - 4k - Cached - Similar pages

[PDF] Layer-by-Layer of Molecular Composites on Quartz and **Nafion**™ for ...
File Format: PDF/Adobe Acrobat - View as HTML
Nafion 117. SPBI. MeOH. MeOH. P2VP. Negatively charged SPBI solution (10 ... Layer-by-Layer Assembly on **Nafion**. **Nafion 117**. **Nafion 117** /(SPBI/P2VP) ...
www.ctfuelcell.uconn.edu/fcic/pdf/fcic_program_oral_6b.5.pdf - Similar pages

[PDF] Microsoft PowerPoint - 621 Livshits.ppt
File Format: PDF/Adobe Acrobat - View as HTML
Conclusion: The water transport in NP-PCMs is 10-20. times higher than in **Nafion 117**. This allows easier. transport of water from the cathode to the anode. ...
www.fuelcellseminar.com/pdf/2004/621%20Livshits.pdf - Similar pages

Transport of alkali metal cations through monoazacrown ether ...
Conditions have been developed for the surface modification of **Nafion 117** cation-exchange membrane by conversion to the sulfonyl chloride form and coupling ...
cat.inist.fr/?aModele=afficheN&cpsidt=3131290 - Similar pages

A comparison of methanol permeability in Chitosan and **Nafion 117** ...
This is almost three times lower than the permeability found for **Nafion 117** of(2. 3 ′ 0. 2) x 10 - 6 cm 2 /s at the same methanol concentration ...
cat.inist.fr/?aModele=afficheN&cpsidt=16150337 - Similar pages
[More results from cat.inist.fr]

Nanophase-Segregation and Transport in **Nafion 117** from Molecular ...
To study such properties, we carried out molecular dynamics (MD) simulations of **Nafion 117** using two extreme monomeric sequences: one very blocky and other ...
pubs.acs.org/cgi-bin/abstract.cgi/jpcbfk/2004/108/i10/abs/jp036842c.html - Similar pages

[PDF] Electrochemical and microscopic characterisation of platinum ...
File Format: PDF/Adobe Acrobat
Platinum-coated **Nafion 117** structures were characterised using ... roughness of **Nafion 117**. Platinum surface areas achieved were higher than the values ...
www.rsc.org/delivery/_ArticleLinking/DisplayArticleForFree.cfm?

doi=a803310b&JournalCode=AN - Similar pages

[PDF] Novel modification of **Nafion 117** for a MEMS-based micro direct ...
File Format: PDF/Adobe Acrobat
membrane **Nafion**. R. **117** to produce an improved polymer electrolyte ... [19] Hobson L J et al 2001 Modified **Nafion 117** as an improved ...
www.iop.org/EJ/S/3/743/YksCO7iVw5YkMLsgIIFSBQ/article/0960-1317/16/9/S09/jmm6_9_s09.pdf - Similar pages

Result Page: 1 2 3 4 5 6 7 8 9 10 **Next**

---

nafion 117 Search

Search within results | Language Tools | Search Tips | Dissatisfied? Help us improve

Google Home - Advertising Programs - Business Solutions - About Google

Tuesday, 1 November 2005 - 5:15 PM
258g

Stability and Performance of Nafion-117 Membranes for the Concentration of Hi/Water and Hi/Water/Iodine Mixtures

Frederick F. Stewart and Christopher J. Orme. Chemical Sciences, Idaho National Laboratory, P.O. Box 1625, Idaho Falls, ID 83415-2208

Thermochemical water splitting processes for generating hydrogen have been researched for at least thirty years in which over one-hundred chemical cycles have been proposed that use heat and/or electrochemistry to split water into hydrogen and oxygen. Proposed heat sources include nuclear reactors and solar reflectors. One of the most promising cycles is the Sulfur-Iodine (S-I) process, where aqueous HI is thermochemically decomposed into H2 and I2 at approximately 350 degrees Celsius. Regeneration of HI is accomplished by the Bunsen reaction (reaction of SO2, water, and iodine to generate H2SO4 and HI). Furthermore, SO2 is regenerated from the decomposition of H2SO4 at 850 degrees Celsius yielding the SO2 as well as O2. Thus, the cycle actually consists of two concurrent oxidation-reduction loops. As HI is regenerated, co-produced H2SO4 must be separated so that each may be decomposed. Current flowsheets employ a large amount (~83 mol% of the entire mixture) of elemental I2 to cause the HI and the H2SO4 to separate into two phases. Removal of water from this system has the direct result of lowering the required quantity of I2, thus reducing the amount of material that must be physically moved within and S-I plant. Recent efforts at the INL have concentrated on applying pervaporation through Nafion-117 membranes for the removal of water from HI/water and HI/Iodine/water feedstreams. In pervaporation, a feed is circulated at low pressure across the upstream side of the membrane, while a vacuum is applied downstream. Selected permeants sorb into the membrane, transport through it, and are vaporized from the backside. Thus, a concentration gradient is established, which provides the driving force for transport. In this work, membrane separations have been performed at temperatures as high as 132 degrees Celsius. Transmembrane fluxes of water are commercially competitive (~200 g/m2h) and separation factors ([HIfeed]/[HIpermeate]) have been measured as high as 500. All membranes studied exhibited no degradation in membrane performance during use.

See more of #258 - Developments in Thermochemical and Electrolytic Routes to Hydrogen Production: Part II (14008)
See more of Nuclear Engineering Division

See more of The 2005 Annual Meeting (Cincinnati, OH)

Electrochemical and microscopic characterisation of platinum-coated perfluorosulfonic acid (Nafion 117) materials†

The Analyst

Sally-Ann Sheppard,[a]† Sheelagh A. Campbell,[a] James R. Smith,[a] Grongar W. Lloyd,[a]§ Thomas R. Ralph[b] and Frank C. Walsh[a]*

[a] *Applied Electrochemistry Group and Scanning Probe Microscopy Laboratory, School of Pharmacy and Biomedical Sciences, University of Portsmouth, St. Michael's Building, White Swan Road, Portsmouth, UK PO1 2DT*
[b] *Johnson Matthey Technology Centre, Blount's Court, Sonning Common, Reading, UK RG4 9NH*

Received 1st April 1998, Accepted 28th July 1998

Platinum-coated Nafion 117 structures were characterised using electrochemical measurements of platinum surface area and a number of microscopy techniques. The morphology and composition of the platinum deposits were related to their preparation conditions in terms of platinum salt concentration, electrolyte flow and the surface roughness of Nafion 117. Platinum surface areas achieved were higher than the values predicted for ideal spherical platinum particles of average diameter. This is due to a fine microstructure, which realises much smaller platinum particles than average (down to about 50 nm) allied to the geometry produced by their clustering to form nodules (about 0.1–1.5 μm diameter micro-nodules and about 3–5 μm macro-nodules). Adherent platinum deposits with high surface areas were promoted by using roughened Nafion 117 membranes and enhancing the mass transport of chloroplatinate and tetraborohydrate ions by magnetic stirring of the electrolyte. A flow cell produced much more reproducible platinum-coated Nafion 117 structures. At best, platinum surface areas of 30–50 $m^2\ g^{-1}$ Pt were achieved at platinum penetration depths of 5–30 μm into the membrane surface.

Introduction

Fluorocarbon ion-exchange membranes coated or laminated to an electrocatalyst layer have become essential components in many electrochemical devices, including proton exchange membrane fuel cells,[1] electrolysis cells[2] and more recently a wide range of sensor devices. For example, an amperometric flow cell incorporating a Pt/Nafion sensor electrode has been successfully used for the amperometric determination of quinones, amines and phenols in aqueous solution and also for hydrazine, hydroquinone, oxalic acid, ascorbic acid and tetracyanoquinodimethane (TCNQ).[3]

DuPont first developed perfluorinated membranes in the early 1960s under the trade-name Nafion. These ion-exchange membranes[4] are copolymers of tetrafluoroethylene and perfluorinated vinyl ethers containing terminal sulfonyl fluoride groups. Such terminal groups are then treated to produce the proton conducting $-SO_3H$ (or $-CO_2H$) groups. The ionomeric structure and properties of ionomers such as Nafion have been discussed in detail elsewhere.[4-11] Nafion is frequently used in fuel cell and electrolysis applications as a result of an excellent chemical and mechanical stability allied to a high ionic conductivity.[12]

Nafion ion-exchange materials produce highly acidic environments as a consequence of the sulfonic acid groups located within the micelle structure.[7] Thus noble metals (most notably platinum) or their oxides are often the electrocatalysts of choice for coating or laminating to the solid polymer electrolyte (SPE).[13] Since noble metal coated SPEs are high cost materials, for the majority of applications low noble metal loadings are required to limit costs. Further, at such loadings, it is important to maximise the active metal surface area to achieve a high metal dispersion on the SPE to promote the desired reaction(s). Good adhesion of the electrocatalyst to the membrane is also necessary to reduce ohmic losses and to support the high mechanical stresses produced during operation. Such stresses arise due to dimensional changes in the membrane during hydration, dehydration and gas evolution, which often accompany the main reaction(s) in electrosynthesis applications.

There are several methods of depositing metal coatings on membrane surfaces, notably mechanically pressing,[14] electrochemical deposition[15,16] and chemical deposition.[17,18] In this study, a chemical reduction route, first reported by Takenaka and co-workers,[17,18] was used to deposit platinum on one side of a Nafion 117 membrane.

In this method, solutions of platinum anions, such as chloroplatinate ($PtCl_6^{2-}$), and a reducing agent, typically tetrahydroborate ion (BH_4^-), are exposed to opposite sides of a stationary SPE membrane. BH_4^- ions continuously penetrate the membrane and come into contact with $PtCl_6^{2-}$ ions on the opposite membrane face, at which point the platinum ions are reduced to platinum metal at the membrane surface according to the redox reactions:

$$PtCl_6^{2-} + 4e^- \rightarrow Pt + 6Cl^- \quad (1)$$

$$BH_4^- + 3H_2O - 4e^- \rightarrow BO_3^{3-} + 2H_2 + 6H^+ \quad (2)$$

to give the overall process:

$$PtCl_6^{2-} + BH_4^- + 3H_2O \rightarrow Pt + BO_3^{3-} + 6Cl^- + 2H_2 + 6H^+ \quad (3)$$

Here, cyclic voltammetry,[19] atomic force microscopy (AFM),[20] scanning electron microscopy (SEM), transmission electron microscopy (TEM) and electron probe microanalysis (EPMA)[21] were used to characterise platinum-coated Nafion 117 membranes under a variety of synthesis conditions.

† Presented at EIRELEC '98, Howth, Co. Dublin, Ireland, March 26–28, 1998.
‡ Present address: INCO Europe Ltd., Acton Refinery, North Acton, London, UK NW10 6SN.
§ Present address: GL Instruments, 5 Chichester Walk, Banbury, Oxford, UK OX16 7YT.

Experimental

The Nafion 117 membrane (nominal thickness 178 μm, Sigma–Aldrich, Dorset, UK) was boiled in de-ionised water for 2 h prior to platinum deposition. A circular disc of the protonated form of Nafion 117 (6.25 cm^2) was mounted vertically between polypropylene flanges closed at one end to accommodate electrolyte. One membrane face was exposed to 25 cm^3 of H_2PtCl_6 (AR grade, Fisher Scientific UK, Loughborough, UK) and the opposite face was simultaneously exposed to 90 cm^3 of 0.1 mol dm^{-3} $NaBH_4$ (SLR grade, Fisher Scientific UK) in 1 mol dm^{-3} NaOH (SLR grade, Fisher Scientific UK). The reaction time was typically limited to 3 h at 295 K. Surface roughening of Nafion 117 was achieved by abrasion with 1200 grade silicon carbide paper prior to placing it in the deposition cell. The deposition process created large amounts of hydrogen [reaction (3)] which needed to be removed to minimise the effect on the platinum deposition. This was achieved by agitating the electrolyte either through manual shaking of the cell at regular (10–15 min) intervals, by magnetically stirring the electrolyte or by placing the cell in a mechanical shaker. Prior to electrochemical studies, the Pt/Nafion samples were soaked for approximately 16 h in 1 mol dm^{-3} H_2SO_4 (AR grade, Fisher Scientific UK) at 295 K to leave the membrane in a hydrated, acid form.

In a modified procedure, hydrogen was removed in a controlled manner using a flow-through cell (Fig. 1). The cell was machined from four blocks of polypropylene (each 3 cm wide × 5 cm long × 1 cm thick). The inner polypropylene blocks formed the electrolyte channels. The H_2PtCl_6 and $NaBH_4$ flow channels were separated by the Nafion 117 membrane, exposing a membrane surface area of 2.35 cm^2. Silicone rubber gaskets were placed between each of the four blocks to prevent leakage. The cell was held together with six brass tie-rods. The H_2PtCl_6 and $NaBH_4$ reservoirs were filled with 80 cm^3 of solution at a temperature of approximately 295 K. The reactant solutions were circulated using two Totton EMP 50/7 pumps. The flow was measured volumetrically before and after each experiment.

The platinum loading on the Pt/Nafion electrodes was determined by the mass difference of the Nafion membrane before and after metal deposition. The membranes were boiled in de-ionised water for 1 h prior to deposition and dried for 20–24 h at 353 K and 740 mmHg to constant mass both before and after deposition.

The real surface area of a catalyst can be orders of magnitude greater than the geometric area. Since adsorption and catalytic reaction rates are based on real surface area, it is important to be able to measure this value. An accepted electrochemical method of estimating the surface area of platinum is to measure the saturated hydrogen coverage, Q_h, of the platinum from a cyclic voltammogram after subtracting the double layer charge. Fig. 2 shows a cyclic voltammogram of a Pt/Nafion surface obtained after 10 h of potential cycling between the limits 0 and 1.5 V *versus* SHE at a potential sweep rate of 40 mV s^{-1} in 1 mol dm^{-3} H_2SO_4 at 295 K. The established features of hydrogen adsorption, hydrogen desorption, double layer charging, oxide formation and oxide reduction are evident as peaks in the voltammogram.[19] It is assumed that each surface platinum atom is associated with one chemisorbed hydrogen atom, allowing the charge corresponding to the area under the strong and weak hydrogen adsorption peaks, Q_h, to be converted to the real electrochemical surface area. When polycrystalline surfaces are considered, the conversion of the adsorption charge to the real surface area is 210 μC cm^{-2} Pt. This value has been generally accepted as a conversion standard:[19]

$$A_{ec} = Q_h/Q_m \quad (4)$$

where A_{ec} is the real electrochemical surface area (cm^2 Pt), Q_h is the saturated hydrogen coverage on the electrode (μC) and Q_m is the electrical charge associated with monolayer adsorption of hydrogen (Q_m = 210 μC cm^{-2} Pt).

The enhancement of real electrochemical surface area, in comparison with a smooth surface, can be described by a roughness factor (cm^2 Pt cm^{-2}):

$$R_F = A_{ec}/A_g \quad (5)$$

where A_{ec} is the real electrochemical surface area (cm^2 Pt) and A_g is the geometric surface area (cm^2), which is a circular disc in the present work.

AFM studies were performed in air under normal atmospheric conditions using a Discoverer TopoMetrix TMX2000 scanning probe microscope (SPM) (TopoMetrix, Saffron Walden, Essex, UK). Samples were mounted on a conductive carbon support and imaged uncoated. A scanner capable of a maximum *x,y,z*- translation of 75 × 75 × 12 μm was used and imaging was performed in contact mode using forces in the range of 1–10 nN. Imaging was restricted to platinum deposits with a surface relief of less than 16 μm owing to limitations in the *z*-range of the scanners piezo-element. Standard profile, silicon nitride tips, mounted on cantilevers of spring constant 0.036 N m^{-1}, were used and the graphic output was displayed on a monitor with a resolution of 400 lines by 400 pixels. Images were levelled by plane fitting and shaded to enhance topographic features; quantitative data were extracted from levelled images.

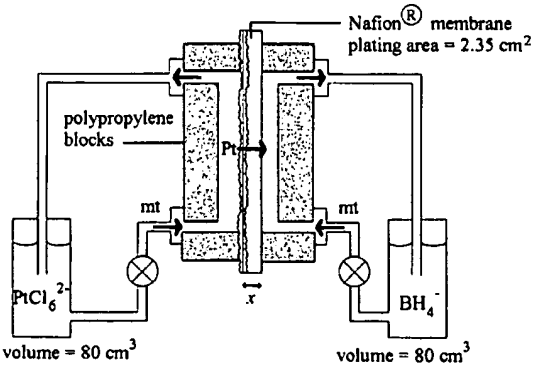

Fig. 1 Schematic diagram of the flow-through cell used to deposit Pt on a Nafion 117 membrane *via* a diffusion process through the membrane involving tetrahydroborate ion reduction of chloroplatinate ion; x = Pt deposit nominal thickness (178 μm); mt = mass transport of species.

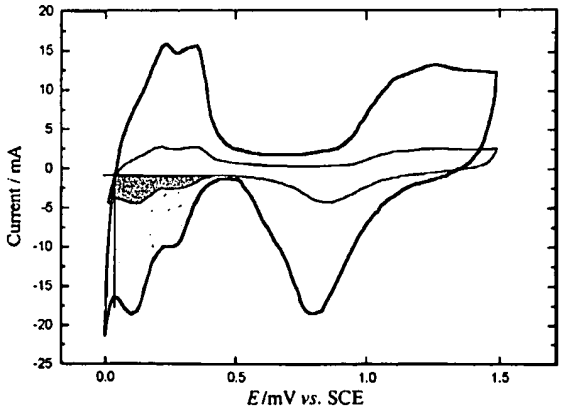

Fig. 2 Cyclic voltammograms of Pt-coated Nafion 117 membrane in 1 mol dm^{-3} H_2SO_4 at 295 K. The inner voltammogram (thin line) was obtained for a low platinum loading (1.2 mg Pt cm^{-2}) and the outer (bold line) for a higher platinum loading (6.4 mg Pt cm^{-2}). The shaded regions on the voltammograms represent the hydrogen adsorption charge, Q_h, used in the surface area measurements. Potential sweep rate: 40 mV s^{-1}.

EPMA was performed using a Camebax SX500 instrument. A section of the Pt/Nafion sample was mounted in resin (Struers Epofit) reinforced with alumina particles. The surface was polished using silicon carbide papers then diamond paste down to a surface roughness of less than 0.1 μm. It was vacuum coated with an approximately 20 nm thickness of carbon to provide an electrically conductive surface. The sample was examined using a beam current of 20 nA and an accelerating voltage of 20 kV. For each Pt/Nafion sample, a peak and background pair of line scans was obtained across the platinum deposit and into the membrane. For the uncoated membrane, a peak and background pair of line scans was run across a portion of the surface. The background signals were subtracted from the peak signals to produce peak-background corrected line scans for platinum and fluorine.

SEM was performed on a Lieca Electron Optics S250 instrument using an accelerating voltage of 20 kV. The Pt/Nafion samples were mounted on a specimen grid and cooled in liquid nitrogen to 77 K and cut with a blade to examine cross-sections. Secondary and backscattered electron micrographs were obtained. TEM utilised a Philips EM400T electron microscope using an acceleration voltage of 100 kV with bright- and dark-field illumination. The Pt/Nafion samples were supported on carbon-coated grids.

Results and discussion

Effect of chloroplatinic acid concentration on platinum deposition

The mass of platinum deposited and the platinum surface area were mainly affected by the reactant concentration, the flux of the diffusing reactants, the deposition time and the temperature. In the first experiments, the H_2PtCl_6 concentration was treated as a major variable. The other variables were kept constant, with manual shaking of the cell initially used to remove hydrogen gas bubbles produced during the deposition process [reaction (3)].

Fig. 3(a) shows the effect of H_2PtCl_6 concentration on the mass of platinum deposited. This increased with H_2PtCl_6 concentration, although the relationship was non-linear with the platinum loading increasing only slightly at higher H_2PtCl_6 levels. The roughness factor, which is the ratio of real electrochemical surface area to geometric area, also increased with H_2PtCl_6 in a non-linear fashion, as shown in Fig. 3(b).

In Fig. 3(c), the results from Fig. 3(a) and (b) are correlated in the form of a roughness factor *versus* platinum-loading plot. Again, a non-linear relationship is evident and there is a relatively large region between 1.2 and 3.5 mg Pt cm^{-2} where the roughness factor increases only slightly with increase in platinum loading. At a platinum loading higher than approximately 3.5 mg Pt cm^{-2}, the roughness factor increases much more steeply. There is a clear trade-off between obtaining high R_F values corresponding to high real electrochemical surface areas and the production of high loading to give thick, expensive platinum deposits.

It is useful to rationalise the experimental roughness factors obtained from hydrogen adsorption coulometry by comparing the data with the predictions of a simple model.[12] The platinum deposit can be naively considered as a homogeneous distribution of smooth, non-porous, spherical particles, each of diameter d (cm). The specific surface area, S (cm^2 g^{-1} Pt), is then given by

$$S = 6/\rho d \quad (6)$$

where ρ is the density of platinum (21.41 g cm^{-3}). The specific surface area may also be related to the real and geometric values of area (A_r and A_g) and the platinum loading, W (g Pt cm^{-2}), by

$$S = (A_r/A_g)(1/W) \quad (7)$$

Since in this study A_{ec} is used to measure A_r, the roughness factor can be described as

$$R_F = SW \quad (8)$$

The selection of an appropriate value for d is difficult as microscopy shows that a wide distribution of platinum particle sizes exists. For the purposes of calculation, 100 nm may be taken as an average particle diameter measured in SEM, AFM and TEM images. Application of eqn. (6) to calculate S and eqn. (8) to give the theoretical R_F *versus* W relationship produces the dotted straight line shown in Fig. 3(c). The experimental data provide roughness factors that are considerably higher than the predicted values. This is illustrated by the model predictions shown by the dashed lines in Fig. 3(c), which indicate that a much better fit is obtained for platinum particle diameters below 50 nm. The simple model cannot, however, accommodate the rapid rise in R_F at high platinum loadings, which corresponds to an increase in the specific surface area of the deposit.

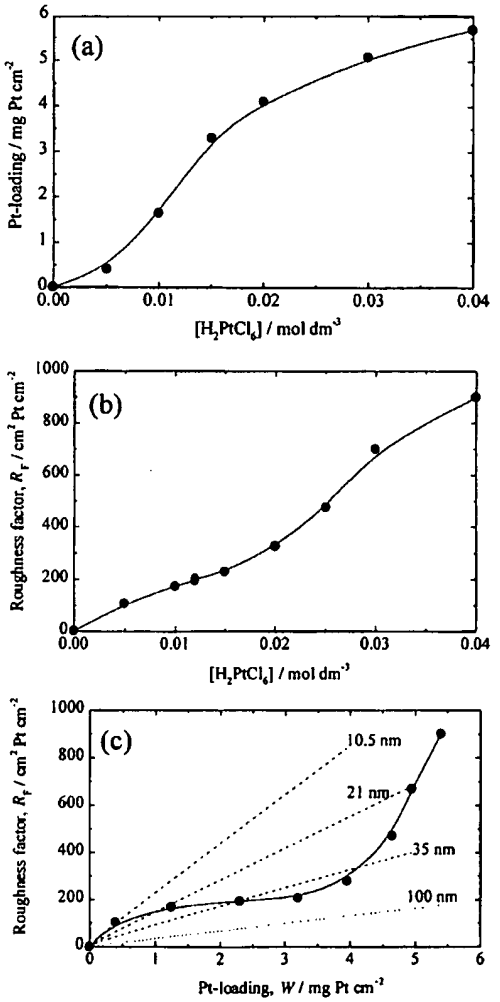

Fig. 3 Relationship between chloroplatinic acid concentration, platinum loading and roughness factor. Deposition conditions: 0.1 mol dm^{-3} $NaBH_4$ in 1 mol dm^{-3} NaOH; 3 h deposition time; T = 295 K; Nafion 117 surface not roughened prior to platinising; manual shaking employed. (a) Dependence of platinum-loading on chloroplatinic acid concentration; (b) dependence of roughness factor on chloroplatinic acid concentration; (c) roughness factor as a function of platinum loading for the data in (a) and (b). The slope of the curve represents the specific surface area of the platinum deposit. The dotted line shows the predictions of a simple model, assuming deposition of smooth, non-porous, homogeneous, spherical particles of Pt having a diameter of 100 nm. The dashed lines show the model predictions for a range of Pt particle diameters.

Investigating the morphology of the platinum deposit highlighted the reason for the high R_F values. Fig. 4(a) shows a typical scanning electron micrograph of a high platinum loading membrane sample (6.4 mg Pt cm^{-2}) prepared using 0.02 mol dm^{-3} H_2PtCl_6 and 0.1 mol dm^{-3} $NaBH_4$ in 1 mol dm^{-3} NaOH with a 3 h deposition time and manual shaking of the cell. A smooth, 'mud-cracked' surface is evident with macro-nodules 2–4 mm wide on islands of width 40–100 μm formed by the cracks in the deposit. The cracks are approximately 1 μm across and were shown to arise during the deposition process itself, rather than from subsequent drying effects. This cracking, which may be caused by an increase in the internal tensile stress in the deposit, may limit the lifetime of the electrode structure in some applications by allowing liquid electrolyte ingress, thereby undermining the deposit and perhaps promoting membrane degradation. Following cracking early in the deposition process, subsequent layers of platinum grew in the cracks, giving rise to a two-layered structure shown in Fig. 4(b). Backscattered electron imaging showed that the platinum had deposited relatively uniformly across the SPE surface, the nominal deposit thickness being approximately 5 μm.

At a lower platinum loading, the noble metal coating showed similar features. For example, SEM studies were also performed on a relatively low platinum loading surface (1.2 mg Pt cm^{-2}) prepared from 0.01 mol dm^{-3} H_2PtCl_6 and 0.1 mol dm^{-3} $NaBH_4$ in 1 mol dm^{-3} NaOH, with a 3 h deposition time and manual shaking of the cell. As expected, a thin platinum coating was formed. In fact, backscattered electron imaging indicated the average deposit thickness was only 0.2 μm and an incomplete surface coverage of the Nafion membrane was obtained. In the plated regions, macro-nodules, 1.0–2.5 μm wide, were evident on islands of width 100–180 μm divided by cracks typically 2–4 μm across.

Closer examination of the relatively 'flat' regions of the surface of the Pt/Nafion structures (with a surface relief less than 16 μm) using AFM provided further insight into the topography. A typical AFM micrograph of the Pt/Nafion membrane is shown in Fig. 5(a). As evidenced by SEM, the deposit can be considered as a series of macro-nodules typically 0.7–3.2 μm in diameter. In Fig. 5(a), AFM clearly shows, however, that these are made up from micro-nodule assemblies of diameter 0.1–1.5 μm. Most importantly, closer examination by TEM revealed a finer grain structure down to 50 nm diameter. Such findings are comparable to those in studies using an impregnation–reduction technique with a $[Pt(NH_3)_4]^{2+}$ salt.[12] As shown in Fig. 3(c), smaller platinum particles give higher R_F values, but with the Pt/Nafion electrodes, since $d \approx$ 100 nm, it is the fine microstructure allied to the way in which the small (50–100 nm) platinum particles cluster to from complex 3D geometries that produces the high R_F values. Further, the rapid rise in R_F at high platinum loading is probably attributable to the effect of the macro-nodules, evident in Fig. 5(a). Certainly the macro-nodules are more likely to be formed at high platinum loading. They may alter the packing of the fine microstructure in a fashion that increases the specific surface area. This macro-nodule formation may be due to heterogeneity in the membrane structure allowing preferential deposition of platinum at specific membrane sites. Some indication of this is given by the difficulty in reproducing macro-nodule formation, with similar preparation conditions giving platinum deposits having varying numbers of macro-nodules.

In addition to the R_F *versus* W relationship, the adhesion of the deposit is very important. EPMA was used to investigate the location of the platinum. Three distinct regions were found, (i)

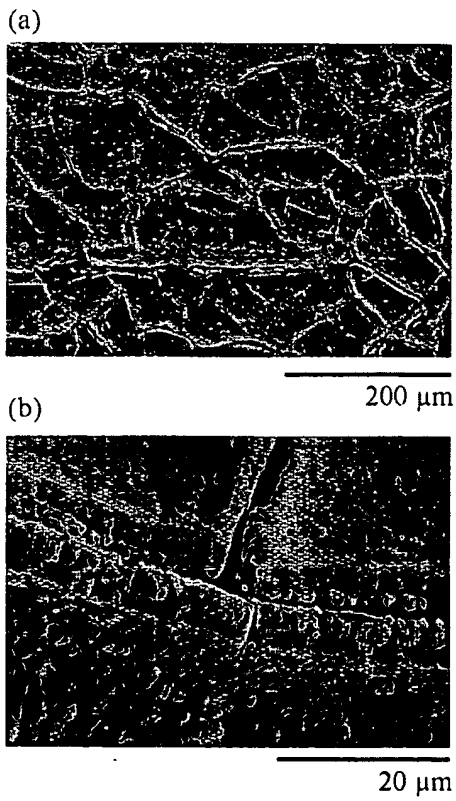

Fig. 4 Scanning electron micrograph of a Pt-coated Nafion 117 membrane surface containing a high platinum loading (6.4 mg Pt cm^{-2}). The deposit was obtained from 0.02 mol dm^{-3} H_2PtCl_6 and 0.1 mol dm^{-3} $NaBH_4$ in 1 mol dm^{-3} NaOH which had been manually shaken during a deposition time of 3 h, T = 295 K with the membrane surface not roughened prior to platinum deposition. Image (b) is an enlarged region of one of the cracked regions seen in image (a).

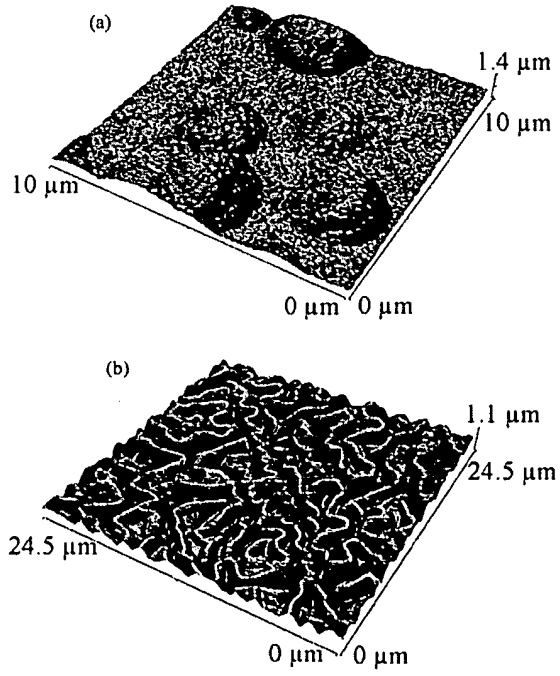

Fig. 5 Atomic force micrographs of Pt-coated Nafion 117 membrane prepared under two different deposition conditions: (a) 0.03 mol dm^{-3} H_2PtCl_6 and 0.1 mol dm^{-3} $NaBH_4$ in 1 mol dm^{-3} NaOH manually shaken during a deposition time of 3 h, T = 295 K, with membrane surface not roughened prior to platinum deposition; (b) structure obtained using a flow-through cell, using 0.02 mol dm^{-3} H_2PtCl_6 (v = 4.3 cm s^{-1}) and 0.1 mol dm^{-3} $NaBH_4$ in 1 mol dm^{-3} NaOH (v = 4.3 cm s^{-1}) over a 4 h deposition time, T = 295 K, with the membrane surface pre-roughened prior to platinum deposition.

an external platinum deposit, (ii) platinum inside the membrane and (iii) very low levels of isolated platinum particles deeper inside the membrane which cannot take part in any reaction. For example, background corrected line scans for platinum and fluorine for a typical Pt/Nafion membrane prepared using 0.02 mol dm^{-3} H_2PtCl_6 and 0.1 mol dm^{-3} $NaBH_4$ in 1.0 mol dm^{-3} NaOH with manual shaking of the cell are shown in Fig. 6. The depth probed was approximately 60 μm into the Nafion 117 material. It is clear that the fluorine level varies considerably in Nafion 117, reflecting the heterogeneous nature of fluorine distribution within the fluorinated polymer network. Fig. 6 shows, however, from the overlap of the platinum and fluorine line scans that platinum has penetrated to a depth of less than 10 μm into the membrane. When the concentration of H_2PtCl_6 was reduced from 0.02 to 0.01 mol dm^{-3}, the top 5–10 μm region of the Pt/Nafion electrodes appeared to be particularly well enriched with platinum. This is in agreement with the findings of Kamasaki *et al.*,[22] who found that by increasing the H_2PtCl_6 concentration, a more adherent deposit could be obtained. As the H_2PtCl_6 concentration increases, more platinum is deposited inside the membrane and hence the adhesion is improved. With manual shaking of the cell, however, the depth of platinum penetration did not exceed 10 μm.

Effect of solution agitation

The electrolyte flow conditions are known to be important during the chemical deposition of platinum.[19,20] Solution agitation is necessary to remove hydrogen gas bubbles from the membrane surface, which interferes with platinum deposition and reduces the roughness factor and specific surface area. Improved agitation also controls adhesion of the precious metal to the membrane surface. The ionic transport of $PtCl_6^{2-}$ and BH_4^- ions within the membrane, which is restricted by electrostatic repulsion of the sulfonic acid groups, is raised. This reduces the concentration polarisation effects within the membrane and extends the penetration depth at which reduction first occurs.[23]

Consequently, alternative methods of solution agitation were investigated. Table 1 summarises the effect of using four types of solution agitation on the platinum loading, roughness factor and specific surface area of the Nafion 117 structures. In these studies, the platinum loading was maintained at a relatively high level (3.9–5.5 mg Pt cm^{-2}) to provide a readily contacted conductive coating of platinum. Table 1 clearly shows that manually shaking the deposition cell at regular intervals produced the lowest R_F value and platinum surface area (7.1 m^2 g^{-1} Pt). This suggests that the hydrogen formed during the reduction process was not efficiently removed from the membrane surface. This inhibited platinum nucleation, resulting in an increased platinum particle size and a lowering of the R_F value and platinum specific surface area. Magnetic stirring of the electrolyte gave a slightly higher deposition rate and an increased R_F value and platinum specific surface area (16.7 m^2 g^{-1} Pt). In this case, the hydrogen was removed more efficiently from the membrane surface, producing more platinum nucleation sites and, hence, a smaller platinum particle size and higher platinum surface area. EPMA also showed a greater degree of platinum penetration of the membrane at a given H_2PtCl_6 concentration. Mechanically shaking the cell showed little increase in the platinum surface area, *i.e.*, even at 5.5 mg Pt cm^{-2} the specific surface area was only 10.3 m^2 g^{-1} Pt. EPMA also showed that at a similar H_2PtCl_6 concentration the platinum was deposited much closer to the surface of the membrane compared with manual shaking of the cell. Mechanically shaking the cell did not provide an efficient method of preparing Pt/Nafion structures.

As a consequence of the success of magnetic stirring, a flow-through cell was designed and built (Fig. 1) to provide a reproducible mass transport regime by controlling the mean linear velocity of the electrolytes during the chemical reduction process.

Fig. 5(b) shows an atomic force micrograph of a platinum-coated Nafion structure (3.8 mg Pt cm^{-2}) obtained after 4 h using the flow-through cell with 0.02 mol dm^{-3} H_2PtCl_6 (v = 4.3 cm s^{-1}) and 0.1 mol dm^{-3} $NaBH_4$ in 1 mol dm^{-3} NaOH (v = 4.3 cm s^{-1}). An extremely regular platinum deposit was obtained. The smooth ripple effect indicates the direction of the solution flow. Typical peak dimensions were 1.5 μm in diameter and 0.27 μm in height. TEM showed a similar fine particle structure down to 50 nm diameter. At platinum loadings in the range 1–5 mg Pt cm^{-2}, comparable R_F values and platinum surface areas were obtained to those achieved by magnetic stirring of the electrolytes (Table 1). Significantly, however, EPMA indicated that at a given platinum loading there was an increased degree of platinum penetration of the

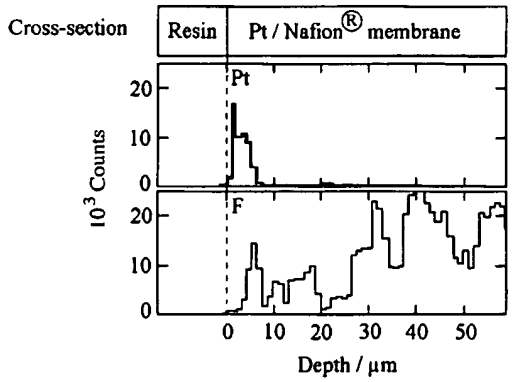

Fig. 6 EPMA traces across a Pt-coated Nafion 117 membrane prepared from 0.02 mol dm^{-3} H_2PtCl_6 and 0.1 mol dm^{-3} $NaBH_4$ in 1 mol dm^{-3} NaOH with the cell mechanically shaken during a deposition time of 3 h, T = 295 K; the membrane surface was not roughened prior to platinum deposition. The vertical axis (distance = zero) corresponds to the surface of the membrane originally in contact with the H_2PtCl_6 solution. Pt (top, thick line) and F (bottom, thin line) spectra have been peak-background corrected.

Table 1 Effect of solution agitation on platinum loading and surface area. Deposition conditions: 0.02 mol dm^{-3} H_2PtCl_6, 0.1 mol dm^{-3} $NaBH_4$ in 1 mol dm^{-3} NaOH; 3 h deposition time; T = 295 K; Nafion 117 membrane surface not roughened

Type of agitation	Pt loading, W/mg Pt cm^{-2}	Roughness factor, R_F/cm^2 Pt cm^{-2}	Specific surface area, S/m^2 g^{-1} Pt
Manual shaking	3.9	278	7.1
Magnetic stirrer	4.1	686	16.7
Mechanical shaker	5.5	568	10.3
Flow-through cell	3.8	640	16.8

Table 2 Effect of surface roughening of Nafion 117 on the platinum surface area. The values in parentheses are for roughened membranes. Deposition conditions: 0.1 mol dm^{-3} $NaBH_4$ in 1 mol dm^{-3} NaOH; 3 h deposition time; T = 295 K; manual shaking employed; Nafion 117 surface pre-roughenened with wet 1200 grade silicon carbide paper

[H_2PtCl_6]/mol dm^{-3}	Pt-loading, W/mg Pt cm^{-2}	Roughness factor, R_F/cm^2 Pt cm^{-2}	Specific surface area, S/m^2 g^{-1} Pt
0.02	3.8	278	7.3
	(3.9)	(997)	(25.6)
0.04	6.7	895	13.4
	(7.1)	(2014)	(28.4)

membrane (up to 5–30 μm at high H_2PtCl_6 concentrations). This produced good adhesion. Most importantly, reproducibility of the platinum deposits was significantly improved over all other forms of solution agitation examined. This is a result of the well defined flow conditions in the cell.[24] It is important to have reproducible flow conditions to produce consistent platinum deposits of high specific surface area with good adhesion.

Effect of surface roughening of the Nafion 117 membrane

In an attempt to improve the roughness factor, specific surface area and adhesion of the platinum deposit, the surface of the Nafion 117 membrane was roughened with silicon carbide paper. Table 2 shows the effect of surface abrasion on the R_F value and platinum surface area at two concentrations of H_2PtCl_6 and a fixed concentration of $NaBH_4$, with manual shaking of the cell. Surface abrasion resulted in an increase in the R_F value and specific platinum surface area by a factor of 2.3–3.5 at a selected platinum loading. This suggests that there was an increase in the number of platinum nucleation sites on the roughened membrane surface, leading to a much reduced platinum particle size. SEM, AFM and TEM analysis confirmed a reduction in the average diameter of the deposited platinum particles to well below the previously observed 100 nm. The topography of the platinum deposit was, however, little changed with the fine microstructure and micro- and macro-nodules on islands formed by cracks observed. EPMA analysis did show a second effect from membrane roughening. More of the platinum deposit was located within the membrane at a given platinum loading. This improved the adhesion of the deposit.

Combining the benefits of the surface roughening of Nafion 117 with those achieved by using the flow-through cell produced the highest quality Pt/Nafion structures achieved in this study. Reproducible platinum deposits with good adhesion, but with higher specific platinum surface areas (30–50 $m^2\ g^{-1}$ Pt) were achieved over a range of platinum loadings. These deposits are much improved over previously reported studies[17,18] of platinum deposition on Nafion 117.

Comparison with conventional electrode technology

It is worth comparing the roughness factors and specific surface areas with those typically achieved using traditional gas diffusion electrode (GDE) technology employed in a number of applications, most notably proton exchange membrane fuel cells.[25,26] Such systems employ carbon supported platinum catalysts impregnated with Nafion membrane electrolyte solution to contact the metal in the electrodes. The GDEs are subsequently hot-pressed to the SPE membrane in applications where this is desired. By using high surface area carbon supports, platinum particle diameters of 2–5 nm are typically found, even after prolonged use.[27] This produces specific surface areas of 60–100 $m^2\ g^{-1}$ Pt at platinum loadings of 40–20% m/m on the carbon support. This translates to R_F values in the range 3000–5000 cm^2 Pt cm^{-2} at a GDE loading of 5 mg Pt cm^{-2} and 300–500 cm^2 Pt cm^{-2} at a more economical GDE loading of 0.5 mg Pt cm^{-2}. At best, the use of roughened Nafion 117 surfaces in a flow-through cell produced a specific surface area of 30–50 $m^2\ g^{-1}$ Pt. This translates to an R_F value of 1500–2500 cm^2 Pt cm^{-2} at an electrode loading of 5 mg Pt cm^{-2} and to 250 cm^2 Pt cm^{-2} at 0.5 mg Pt cm^{-2}. The potentially available platinum surface area is approximately 50% lower in the platinum-coated membrane electrodes. Although higher electrocatalyst surface areas do not necessarily translate to a higher performance as a result of kinetic, ohmic and mass transport losses within the electrode matrix,[27] they do imply a potential benefit.

Conclusions

The preparation conditions influencing the properties of platinum-coated Nafion 117 materials for electrochemical applications were investigated using the procedure of Takenaka and co-workers[17,18] for the chemical deposition of platinum on to the membrane *via* $NaBH_4$ reduction of H_2PtCl_6. Particular attention was given to H_2PtCl_6 concentration, the electrolyte agitation conditions during the chemical deposition and to surface roughening of the Nafion 117 membrane as a pre-treatment.

The practical considerations for an 'ideal' structure include production of a porous deposit, a high surface area of platinum in contact with the Nafion membrane for good electrocatalysis and metal adhesion, with the platinum layer extending outside the membrane so that a current collector can be readily contacted.[2] To achieve this using the $NaBH_4$ reduction of H_2PtCl_6, a high concentration of H_2PtCl_6 should be used, with control of the electrolyte flow conditions and roughening of the Nafion membrane surface. Stirred or mechanically shaken conditions can be used but a flow-through cell using the plane, parallel plate geometry provides a preferred, controlled mass transport regime. The flow-through cell gives rise to a uniform deposit morphology and a controlled and high penetration beneath the Nafion 117 surface. In addition, a high platinum surface area was produced, principally owing to the efficient removal of hydrogen gas bubbles from the membrane surface. Roughening the membrane also raised the platinum surface area by increasing the number of nucleation sites available for platinum deposition. The combination of conditions used produced coherent platinum deposits with platinum surface areas at best around 50% of those achieved using current GDEs with carbon-supported catalysts. Further investigation of membrane pre-treatments and deposition conditions could give rise to improved platinum deposits.

Acknowledgements

Studentship support from the EPSRC (to S.-A.S.) is gratefully acknowledged. Mr. Mike Matthews (JMTC) provided valuable assistance with the EPMA and electron microscopy measurements.

Appendix

Symbols

A_{ec}	Electrochemical surface area	cm^2 Pt
A_g	Geometric surface area	cm^2
A_r	Real surface area	cm^2 Pt
d	Diameter of spherical particles	cm
Q_m	Electrical charge associated with monolayer adsorption of hydrogen	210 μC cm^{-2} Pt
Q_h	Charge associated with saturated hydrogen coverage	μC
R_F	Roughness factor	cm^2 Pt cm^{-2}
S	Specific surface area	$cm^2\ g^{-1}$ Pt
T	Temperature	K
W	Platinum-loading	g Pt cm^{-2}
v	Mean linear flow velocity of electrolyte	cm s^{-1}
ρ	Bulk density of platinum	21.41 g cm^{-3}

References

1 M. Wakizoe, O. V. Velev and S. Srinivasan, *Electrochim. Acta.*, 1995, **40**, 335.
2 P. S. Fedkiw, J. M. Potente and W.-H. Her, *J. Electrochem. Soc.*, 1990, **137**(5), 1451.
3 T. W. Kaaret and D. H. Evans, *Anal. Chem.*, 1988, **60**, 657.
4 T. A. Davis, J. D. Genders and D. Pletcher, *A First Course in Ion Permeable Membranes*, Electrochemical Consultancy, Romsey, 1997.
5 R. S. Yeo and H. L. Yeager, *Modern Aspects Electrochem.*, 1985, **16**, 437.
6 T. D. Gierke, G. E. Munn and F. C. Wilson, *J. Polym. Sci., Part B: Polym. Phys.*, 1981, **19**, 1687.
7 T. D. Gierke and W. Y. Hsu, in *Perfluorinated Ionomer Membranes*, ed. H. L. Yeager and A. Eisenberg, ACS Symposium Series, No. 180, American Chemical Society, Washington, DC, 1982, pp. 283–307.
8 B. Dreyfus, G. Gebel, P. Aldeburt and M. Pineri, *J. Phys. (Paris)*, 1990, **51**, 1341.
9 P. C. Lee and D. Meisel, *J. Am. Chem. Soc.*, 1980, **102**, 5477.
10 T. Xue, J. S. Trent and K. Osseo-Asare, *J. Membr. Sci.*, 1989, **45**, 261.
11 H. L. Yeager and A. Eisenberg, in *Perfluorinated Ionomer Membranes*, ed. H. L. Yeager and A. Eisenberg, ACS Symposium Series, No. 180, American Chemical Society, Washington, DC, 1982, p. 1.
12 F. Delime, J. M. Leger and C. Lamy, *J. Appl. Electrochem.*, 1998, **28**, 27.
13 P. Millet, R. Durand and M. Pineri, *Int. J. Hydrogen Energy*, 1990, **15**(4), 245.
14 R. J. Lawrance and L. D. Wood, *US Pat.*, 4 272 353, 1981.
15 R. Banzinger, H.-J. Christen and S. Stucki, *US Pat.*, 4 396 469, 1983.
16 H. Nagel, *US Pat.*, 4 326 930, 1982.
17 H. Takenaka and E. Torikai, *Kokai Tokyo Koho (Jpn. Pat.)*, 55 38934, 1980.
18 H. Takenaka, E. Torikai, Y. Kawami and N. Wakabaysh, *Int. J. Hydrogen Energy*, 1982, **7**(5), 397.
19 R. Woods, *J. Electroanal. Chem.*, 1981, **9**, 9.
20 G. Binnig, C. F. Quate and C. Gerber, *Phys. Rev. Lett.*, 1986, **59**, 930.
21 M. Andrae, K. Rohrbacher, P. Klein, L. Udvary and J. Wernisch, *Scanning*, 1997, **19**(7), 477.
22 S. Kamasaki, S. Sekido, S. and Y. Miua, *Mem. Fac. Technol. Metropolitan Univ.*, 1988, **38**, 141.
23 L. E. Manring and S. Mazur, *J. Phys. Chem.*, 1986, **90**, 3269.
24 D. W. DeWulf and A. J. Bard, *J. Electrochem. Soc.*, 1988, **135**(8), 1977.
25 E. A. Ticianelli, C. R. Derouin and S. Srinivisan, *J. Electroanal. Chem.*, 1988, **251**, 275.
26 M. S. Wilson and S. Gottesfeld, *J. Electrochem. Soc.*, 1992, **139**(2), L28.
27 T. R. Ralph, G. A. Hards, J. E. Keating, S. A. Campbell, D. P. Wilkinson, M. Davis, J. St.-Pierre, and M. C. Johnson, *J. Electrochem. Soc.*, 1997, **144**(11), 3845.

Paper 8/03310B

Fuel Cell Membrane Shootout Showcases Hydrocarbon Superiority; PolyFuel Takes on Nafion 117 at Fuel Cell Seminar Demo

SAN ANTONIO--Nov. 1, 2004--PolyFuel, Inc., a world leader in engineered membranes for fuel cells, is running a real-time shootout between one of its revolutionary, hydrocarbon-based direct methanol fuel cell (DMFC) membranes, and Du Pont's Nafion 117, at the Fuel Cell Seminar here through November 4. Utilizing absolutely identical test setups that differ only in the membrane, PolyFuel is running demonstrations continuously over the four-day period. In addition, PolyFuel is showcasing publicly for the first time its recently-announced hydrogen membrane for automotive fuel cell applications in a functioning fuel cell test station.

The DMFC comparison -- which includes continuously-updated cumulative results -- shows that PolyFuel's hydrocarbon DMFC membrane has substantially improved performance when compared to the fluorocarbon-based Nafion membrane. In addition, the hydrogen demonstration gives observers a first look at an automotive-focused membrane that operates stably at 95C and 50% air relative humidity, while simultaneously producing "best of breed" power levels -- a performance combination that has never been achieved before with other materials.

Fuel cell membranes, which resemble ordinary plastic wrap, are the critical component that permits electricity to be generated directly from hydrogen or hydrogen-rich fuel sources in cells that can power anything from cellular telephones to laptop computers to automobiles. Direct methanol fuel cells, which utilize readily-available methyl alcohol as fuel, are expected to offer a long-run-time alternative to batteries for mobile electronics applications. Such cells, and their small, exchangeable fuel cartridges, will snap into such devices much as batteries do today. Hydrogen-based fuel cells are believed by many to be the best long-term power solution for motor vehicles as fossil fuels become less available, and as environmental and political concerns escalate.

"The performance of a fuel cell membrane determines whether or not the cell will be practical in any given application," says Dr. Robert F. Savinell, dean of engineering at Case Western Reserve University and George S. Dively professor of engineering. "PolyFuel has achieved a combination of performance characteristics that are impressive, and the benefits of their groundbreaking work will be readily apparent in their demonstration at the Seminar."

Fuel cell membranes -- technically "proton exchange membranes" -- use a catalyst coating such as platinum to coax electrons away from their companion protons in hydrogen atoms in the fuel. The membrane permits the protons to cross through it -- the exchange -- but the electrons cannot. Instead, they flow out the terminal of the fuel cell, through the load to do work, and then back into the opposite side to recombine with protons and oxygen to make water. Water, heat, and in the case of DMFC, carbon dioxide, are the only byproducts of this reaction.

What has proven problematic for fuel cell designers is that existing membranes, particularly the most commonly available perfluorinated or fluorocarbon membranes such as Nafion have several severe limitations.

For example, existing DMFC membranes essentially "leak". The methanol fuel on one side of the membrane crosses over to the air side of the fuel cell, where it creates troublesome excess heat and water. This increases fuel consumption significantly. With higher concentrations of methanol -- desirable from a fuel efficiency and runtime perspective -- the crossover is even worse. In addition, existing DMFC membranes require significant amounts of water to achieve good performance, diluting the concentration of the fuel, which increases the size of the fuel cell and reduces overall energy density.

Existing hydrogen membranes, for their part, suffer from operating range and life limitations. Today for example, they operate comfortably only within a narrow temperature range of 0C to 80C, not low enough to be able to start a car in wintertime, and not high enough to be able to reach full power in summertime. As well, today's fluorocarbon membranes require high levels of

humidification (typically 80% relative humidity (RH) or above), which increases engine size and complexity. Each of these factors makes the material problematic in automotive applications, preventing the fuel cell vehicle from being competitive with today's internal combustion engine vehicles. In addition, fluorocarbon membranes are structurally weak, limiting the in-service lifetime of today's fuel cell engines to well below the automotive requirement of 5000 hours.

PolyFuel's Membranes and the DMFC Membrane Shootout

PolyFuel is the world's first pure-play membrane company with the technology to directly engineer membranes to end-user requirements. Some time ago, its scientists and engineers concluded that fluorocarbon-based membranes would never achieve the cost or performance figures sufficient to yield small, lightweight, and inexpensive fuel cells that could significantly outperform the batteries they were intended to replace, nor live up to the stringent operating requirements that are characteristic of automotive applications.

Instead, the company engineered several new families of membranes based upon hydrocarbon polymers, which PolyFuel has found to be intrinsically cheaper, stronger, and better performing than their fluorocarbon cousins. Two breakthroughs have resulted from this pioneering work -- the PolyFuel DMFC membrane, and the new PolyFuel hydrocarbon membrane technology for automotive hydrogen fuel cells, recently announced (see "PolyFuel Announces Breakthrough Technology Advance for Automotive Fuel Cells," http://www.polyfuel.com/pressroom/press_pr_100504.html, October 4, 2004.)

In the shootout, which PolyFuel calls the "DMFC Challenge Demo," the PolyFuel hydrocarbon DMFC membrane and the Nafion 117 membrane have been built into otherwise identical "brassboard" test setups. The test setups permit observers to easily monitor fuel consumption as well as gross and net power, and wastewater production in real time, during the 20-minute demonstration. In addition, PolyFuel is continuously updating the cumulative results over the 4-day show. Operating conditions for the two setups -- including output current, air, and fuel concentrations -- are identical, as well.

A few feet away, a single cell test setup is demonstrating a working hydrogen fuel cell with the new PolyFuel hydrogen membrane.

Unprecedented Results

Seminar attendees will observe that the PolyFuel DMFC membrane produces 15% more net electrical output than Nafion 117 while consuming 25% less fuel, and does this producing 55-60% less waste water, with 30% less heat, and consuming 55-60% less water. Based upon 110 cc of methanol fuel (about 3.7 US fluid ounces), a laptop computer using an average of 15 Watts could be expected to run eight hours, 35% longer than with the Nafion fluorocarbon membrane.

In regards to the hydrogen membrane, attendees will see stable production of power at "best of breed" levels, with the cell operating at 95C and 50% air RH.

Jim Balcom, president and CEO of PolyFuel puts both the quantitative results of the shootout, and additional benefits of PolyFuel's hydrocarbon membranes, in perspective. "DMFC manufacturers will be able to use a 1/3 smaller stack, with 1/3 less membrane and 1/3 less catalyst," he said. "Additionally, the water recovery requirement, the heat exchange requirement, and the air supply can all be smaller and less complex. And finally, a higher concentration of fuel, and a smaller fuel cartridge, can be used." These results combine, Balcom stated, to yield portable fuel cell systems that are smaller, lighter, less costly, more robust, quieter, and particularly important -- have longer run times -- than previous approaches.

"On the automotive side," he added, "the outstanding performance of our hydrogen membrane technology will allow fuel cell vehicle designers to more easily engineer fuel cell engines that meet the stringent requirements for motor vehicle applications."

PolyFuel's DMFC membranes are being marketed to portable fuel cell manufacturers worldwide. Balcom reports that virtually every leading fuel cell OEM is testing PolyFuel's DMFC membrane, and are reporting exceptional results. In addition, he said, interest in PolyFuel's new hydrogen membrane by automotive fuel cell vehicle manufacturers is strong.

The Fuel Cell Seminar (www.fuelcellseminar.com) is being held November 1-4, 2004 at the Henry Gonzalez Convention Center, San Antonio, Texas, and attracts over 2,500 attendees.

About PolyFuel

PolyFuel is a world leader in engineered membranes that provide breakthrough performance in fuel cells for portable electronic and automotive applications. The state of the art of fuel cells is essentially that of the membrane, and PolyFuel's leading-edge, hydrocarbon-based membranes enable a new generation of fuel cells that for the first time can deliver on the long-awaited promise of clean, long-running, and cost-effective portable power, based upon renewable energy sources.

PolyFuel's unmatched capability to rapidly translate the system-level requirements of fuel cell designers and manufacturers into engineered polymer nano-architectures has led to its introduction of best-in-class hydrocarbon membranes for both portable direct methanol fuel cells and for automotive hydrogen fuel cells. Such capability -- based on PolyFuel's over 150 combined years of fuel cell experience, world-class polymer nano-architects, and a fundamental patent position covering more than 15 different inventions -- also makes PolyFuel an essential development partner and supplier to any company seeking to advance the state of the art in fuel cells. Polymer electrolyte fuel cells built with PolyFuel membranes can be smaller, lighter, longer-running, more efficient, less expensive and more robust than those made with other membrane materials.

PolyFuel was spun out of SRI International (formerly Stanford Research Institute) in 1999, after 14 years of applied membrane research. The company is based in Mountain View, California, and is privately held. Investors include Mayfield, Ventures West, CDP Capital - Private Equity, Technology Partners, Intel Capital, Chrysalix Energy, Conduit Ventures, KTB Ventures, Hotung Venture Partners, Yasuda Enterprise Development, and BiNEXT, a part of the Daesung Group.
